Reverse genetics with a full-length infectious cDNA of severe acute respiratory syndrome coronavirus

Boyd Yount*†, Kristopher M. Curtis*†, Elizabeth A. Fritz‡, Lisa E. Hensley‡, Peter B. Jahrling‡, Erik Prentice§, Mark R. Denison§, Thomas W. Geisbert‡, and Ralph S. Baric*¶‖

*Departments of Epidemiology and Microbiology and Immunology and ¶Carolina Vaccine Institute, University of North Carolina, Chapel Hill, NC 27599-7435; ‡U.S. Army Medical Research Institute of Infectious Diseases, Fort Detrick, MD 21702; and §Departments of Pediatrics and Microbiology and Immunology, Elizabeth B. Lamb Center for Pediatric Research, Vanderbilt University Medical Center, Nashville, TN 37232

Communicated by Peter Palese, Mount Sinai School of Medicine, New York, NY, August 29, 2003 (received for review August 7, 2003)

A previously undescribed coronavirus (CoV) is the etiologic agent responsible for severe acute respiratory syndrome (SARS). Using a panel of contiguous cDNAs that span the entire genome, we have assembled a full-length cDNA of the SARS-CoV Urbani strain, and have rescued molecularly cloned SARS viruses (infectious clone SARS-CoV) that contained the expected marker mutations inserted into the component clones. Recombinant viruses replicated as efficiently as WT virus and both were inhibited by treatment with the cysteine proteinase inhibitor (2*S*,3*S*)-transepoxysuccinyl-L-leucylamido-3-methylbutane ethyl ester. In addition, subgenomic transcripts were initiated from the consensus sequence ACGAAC in both the WT and infectious clone SARS-CoV. Availability of a SARS-CoV full-length cDNA provides a template for manipulation of the viral genome, allowing for the rapid and rational development and testing of candidate vaccines and therapeutics against this important human pathogen.

Severe acute respiratory syndrome (SARS) is a life-threatening respiratory disease that probably originated in Guangdong Province, China, in the fall of 2002 (1, 2). A previously undescribed coronavirus (CoV), isolated from febrile and dying patients, is the etiologic agent responsible for the disease (3–8). SARS-CoV infection is associated with overall case fatality rates thought to approach ≈14–15%, with selected populations being at increased risk (www.who.int/csr/sars/archive/2003_05_07a/en). SARS-CoV infected >8,000 individuals and caused >800 deaths (www.who.int/csr/sars/en) before aggressive infection control measures successfully contained the scope of the outbreak. Despite intensive efforts, no effective antiviral treatments against SARS have been described.

CoVs, members of the order Nidovirus, contain the largest single-stranded, positive-polarity RNA genome in nature and are divided into three main serogroups, group I CoVs: transmissible gastroenteritis virus (TGEV) and human CoV 229E (HCV-229E), group II: mouse hepatitis virus (MHV) and bovine CoV, and group III: infectious bronchitis virus (IBV). Although initial phylogenetic comparisons suggested that SARS-CoV may represent the prototype strain of group IV (6, 8–10), more recent analyses characterized SARS-CoV as an early split-off among group II (11). The SARS-CoV genomic RNA is ≈29,700 bp in length and has several large ORFs encoded in subgenomic and full-length mRNAs (8–10). The subgenomic mRNAs comprise a nested set of 3′-coterminal molecules in which the leader RNA sequences, encoded at the 5′ end of the genome, are joined to body sequences at distinct transcription regulatory sequences containing a highly conserved consensus sequence (CS). The exact SARS CS has been predicted as either CUAAAC or AAACGAAC (8, 9). The SARS-CoV genome-length RNA is likely encapsidated by multiple 50-kDa nucleocapsid proteins (N) (8). As with other CoVs, the virion contains several viral structural proteins including the spike glycoprotein of ≈140 kDa (S), a 23-kDa membrane glycoprotein (M), and an ≈10-kDa E protein.

The CoV gene 1, or replicase gene, comprises two-thirds of the genome. MHV and SARS-CoV contain two overlapping ORFs, ORF1a and ORF1b, which are connected by a ribosomal frame shift (Fig. 1*A*). In MHV, three proteinases, papain-like proteinases 1 and 2 (11–14) and 3C-like proteinase, mediate cleavage of the polyproteins into at least 15 mature proteins (11, 15). The SARS virus replicase gene is predicted to encode only the papain-like proteinase 2 and 3C-like proteinases (6, 7).

Continuous polyprotein processing is crucial for ongoing virus transcription; therefore, MHV replication is sensitive to protease inhibitors that prevent replicase processing (12). Additional functions have been predicted for proteins processed from the replicase polyprotein, including an RNA-dependent RNA polymerase (pol), an RNA helicase (hel), a capping enzymatic activity, and several putative RNA-processing enzymatic activities (6, 11, 16). In this article, we recover recombinant SARS-CoV from a full-length cDNA of the genome by using an approach that will allow for rapid genetic analysis of SARS-CoV protein functions and replication.

Experimental Procedures

Virus and Cells. The Urbani and Canadian strains (Tor-2 and Tor-7) of SARS-CoV were propagated in VeroE6 cells in MEM supplemented with 10% FCS, kanamycin (0.25 μg/ml), and gentamyacin (0.05 μg/ml) at 37°C in a CO_2 incubator. Cultures of VeroE6 cells were infected at a multiplicity of infection of 0.1 for 30 min, washed, and titered by plaque assay. At 1 h after infection, some cultures were treated with the cysteine protease inhibitor (2*S*,3*S*)-transepoxysuccinyl-L-leucylamido-3-methylbutane ethyl ester (E64-d) at a concentration of 500 μg/ml. Virus plaques were visualized by neutral red staining at 2 d after infection. MHV-A59 was grown as described in the presence or absence of E64-d (12, 17).

Strategy for Cloning the SARS-CoV cDNAs. Reverse transcription was performed by using SuperScript II, oligodeoxynucleotide primers, and intracellular RNA from SARS-infected cultures (17, 18). The cDNA was denatured for 2 min at 94°C and amplified by PCR with Expand Long TAQ polymerase (Roche Molecular Biochemicals) for 25 cycles at 94°C for 30 sec, 58°C for 25–30 sec, and 68°C for 1–7 min. The amplicons were cloned into Topo II TA (Invitrogen) (SARS subclones D–F) or in pSMART vectors (Lucigen, Middleton, WI) (SARS subclones A–C). All cDNAs were assembled as CSs based on independent sequence analysis of four to seven sibling clones and the reported

Abbreviations: CoV, coronavirus; SARS, severe acute respiratory syndrome; icSARS, infectious clone SARS; E64-d, (2*S*,3*S*)-transepoxysuccinyl-L-leucylamido-3-methylbutane ethyl ester; TGEV, transmissible gastroenteritis virus; MHV, mouse hepatitis virus; IBV, infectious bronchitis virus; CS, consensus sequence.

†B.Y. and K.M.C. contributed equally to this work.

‖To whom correspondence should be addressed. E-mail: rbaric@email.unc.edu.

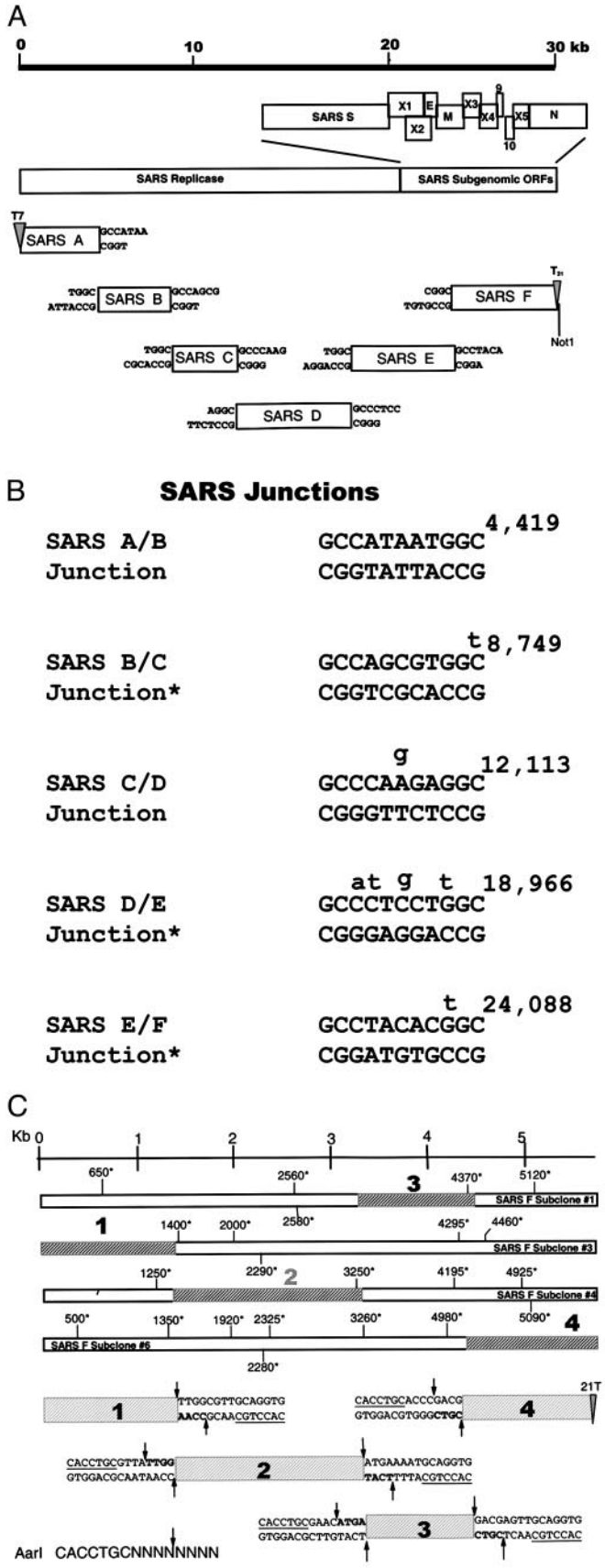

Fig. 1. Assembly of a full-length SARS-CoV cDNA. (*A*) Structure of the SARS-CoV genome (8, 9). The SARS Urbani ≈29,727-bp genome contains 10 or more ORFs, which are expressed from full-length and subgenomic-length mRNAs (8). (*B*) Several *Bgl*I-interconnecting junctions were inserted between the component clones to allow assembly of a full-length cDNA. Lowercase letters represent WT sequence and numbers represent nucleotide positions in genome. (*C*) ''No see'm'' *Aar*I repair of SARS sibling clones. Asterisks represent sites of mutation. Numbers in bold represent portions of sibling clones that were assembled into a consensus SARS F subclone.

Urbani sequence (8). The following primers were used in the isolation of the SARS A subclone (forward, tactaatacgactcactatagatattaggtttttacctacccagg-1, reverse, acaccatagtcaacgatgcc-4452); SARS B subclone (forward, gcctatatgcatggatgttagat-4359, reverse, tgaaccgccacgctggctaaacc-8727); SARS C, subclone (forward, agccagcgtggcggttcatac-8710, reverse, aggcctcttgggcagtggcataag-12085); SARS D subclone (forward, actgcccaagatgcctatgagc-12070, reverse, cagccaggagggcagacttcacaacc-18939); SARS E subclone (forward, gtctgccctcctggctgataagtttccag-18923, reverse, gagcagccgtgtaggcagcaat-24066); and SARS F subclone (forward, attgctgcctacacggctgctc-24045 reverse, $(ttt)_7$gtcattctcctaagaagc-29710).

To repair sibling clones, primer pairs were designed that contained a class IIS restriction enzyme, like *Aar*I. By using high fidelity PCR, the consensus portions of different sibling clones were amplified, digested with *Aar*I, and ligated into plasmid. The *Aar*I junctions were designed to seamlessly link consensus fragments, resulting in the production of a full-length cDNA fragment for each of the various SARS cDNA subclones (17). By using an automated Applied Biosystems DNA sequencer, two to three candidate DNAs were sequenced to identify the consensus clone.

Systematic Assembly of a Full-Length SARS-CoV cDNA. The SARS A–F inserts were restricted, separated through 0.8% agarose gels, visualized with a darkreader lightbox (Clare Chemical Research, Dolores, CO), excised, and purified by using the Qiaex II DNA purification kit. The SARS A + B, C + D, and E + F subclones were ligated overnight and isolated (17, 18). The SARS AB + CD + EF cDNAs were ligated overnight at 4°C, phenol/chloroform extracted and precipitated. Transcripts were generated *in vitro* (TmMessage mMachine, Ambion) as described by the manufacturer with certain modifications (17). For SARS N transcripts, 1 μg of plasmid DNA encoding the N gene (primer: 5′-nnggcctcgatggccatttaggtgacactatagatgtctgataatggaccccaatc-3′ and reverse primer (5′-nnnttttttttttttttttttttttttttttatgcctgagttgaatcagcag-3′) were transcribed by SP6 RNA polymerase with a 2:1 ratio of cap analog to GTP.

Transfection of Full-Length Transcripts. RNA transcripts were added to 800 μl of the BHK cell suspension (8.0×10^6), and three electrical pulses of 850 V at 25 μF were given with a Gene Pulser II electroporator (Bio-Rad) (17, 18). The BHK cells were seeded with $1.0–2.0 \times 10^6$ VeroE6 cells in a 75-cm^2 flask and incubated at 37°C for 2 d. Virus progeny were then purified by plaque assay. For fluorescent Ab staining, cells were washed in PBS and incubated with goat serum for 20 min at room temperature. The cells were washed, incubated with a 1:200 dilution of MHV polyclonal antiserum that cross reacts with the SARS N protein, and then incubated in Alexa 488 diluted 1:400 for 30 min. The cells were fixed in 10% neutral, phosphate-buffered formalin for 24 h, rinsed for 30 min, and visualized under a fluorescent microscope.

Detection of Marker Mutations Inserted in Infectious Clone (ic)SARS-CoV. Intracellular RNA was isolated from either WT or icSARS-CoV-infected cells at 24 h after infection. After RT-PCR, we obtained a 1668-nt amplicon (nucleotide positions 1007–2675) spanning the *Bgl*I site at position 1557 that had been ablated in the icSARS-CoV component clones, but not WT SARS-CoV. Other PCR products included a 799-nt amplicon spanning the

SARS-CoV B/C junction (nucleotide positions 8381–9180), a 544-nt amplicon (nucleotide positions 11721–12265) spanning the SARS-CoV C/D junction, a 652-nt amplicon spanning the SARS-CoV D/E junction, and a 1594-nt amplicon (nucleotide positions 23665–25259) spanning the SARS-CoV E/F junction. The 1594-nt SARS E/F junction-containing amplicon was subcloned and sequenced.

RT-PCR of Leader-Containing Transcripts. Leader-containing amplicons were obtained from WT and icSARS-CoV-infected cells by using primers at the 3′ end of the genome (5′-ttttttttttttttttttttt-tgtcattctcctaagaagc^{29710}-3′) or in the X5 or X3 ORFs (5′-ttaattaattaatttgttcgtttatttaaaacaaca^{28091}′-3′, 5′-ttaattaattatggata-atctaactccataggttct^{27238}-3′) and in the SARS leader RNA sequence at the 5′ end of the genome (5′-aaagccaaccaacctcgatc-3′; nucleotides 26–35). Leader-containing amplicons were subcloned into TopoII vectors and sequenced.

Results

Assembly of SARS Full-Length cDNAs. Rapid response and control of exigent emerging pathogens requires an approach to quickly generate full-length cDNAs from which molecularly cloned viruses are rescued, allowing for genetic manipulation of the genome. Full-length cDNAs were isolated for TGEV, HCoV-229E, IBV, and MHV-A59 by using a variety of approaches (17–21). Our strategy includes a panel of cDNAs spanning the entire CoV genome, which can be systematically and directionally assembled into a genome-length cDNA by *in vitro* ligation (17, 18). The SARS genome was cloned as six contiguous subclones that could be systematically linked by unique *Bgl*I restriction endonuclease sites (Fig. 1). *Bgl*I is a class IIS restriction endonuclease that cleaves the symmetrical sequence GCCNNNN↓NGGC but leaves 64 different asymmetrical ends. Consequently, pairs of contiguous subclones encoded junctions that allow unidirectional assembly of intermediates into a full-length cDNA. As shown in Fig. 1*A*, two *Bgl*I junctions were derived from sites encoded within the SARS-CoV genome at nucleotide positions 4373 (A/B junction) and 12065 (C/D junction) (8–10). A third *Bgl*I site at nucleotide position 1577 was removed and new *Bgl*I sites were inserted by the introduction of silent mutations into the SARS-CoV sequence at nucleotide 8700 (B/C junction), nucleotide 18916 (D/E junction), and at nucleotide 24040 (E/F junction) (Fig. 1*B*). As described with MHV and TGEV, SARS-CoV sequence toxicity was circumvented by disruption of toxic domains and the use of stable cloning vectors (17). The resulting cDNAs include SARS A (nucleotides 1–4436), SARS B (nucleotides 4344–8712), SARS C (nucleotides 8695–12070), SARS D (nucleotides 12055–18924), SARS E (nucleotides 18907–24051), and SARS F (nucleotides 24030–29736) subclones. The SARS A subclone contains a T7 promoter and the SARS F subclone terminates in 21Ts, allowing for *in vitro* transcription of capped, polyadenylated transcripts.

Numerous mutations were noted in each of the four to seven sibling subclones encoding a given SARS cDNA fragment (Fig. 1*C*). To rapidly assemble consensus clones, we used class IIS restriction endonucleases that cut at asymmetric sites and leave asymmetric ends. These enzymes generate strand-specific unique overhangs that allow the seamless ligation of two cDNAs with the concomitant loss of the restriction site (17). As illustrated with the SARS F sibling subclones, primers were designed that contained terminal *Aar* I (CACCTGCNNNN↓NNNN) sites that flanked each of the various consensus portions of different sibling clones. In some instances (amplicons 3 and 2 in sibling clones 1 and 4, respectively), the primers repaired specific mutations located near the ends of a given amplicon (Fig. 1*C*). The combination of high-fidelity PCR, oligonucleotide primer repair, and the seamless ligation of sequence fragments(17), rapidly generated Urbani consensus cDNAs for each of the SARS A, B, C, D, E, and F subclones (Fig. 1*C*). Silent changes retained in the full-length construct included an A to G change at nucleotide position 6460, a T to C at nucleotide position 14178, a T to C at nucleotide position 15740, a C to T at nucleotide position 19814, an A to G at nucleotide position 20528, and a T to C at nucleotide position 20555.

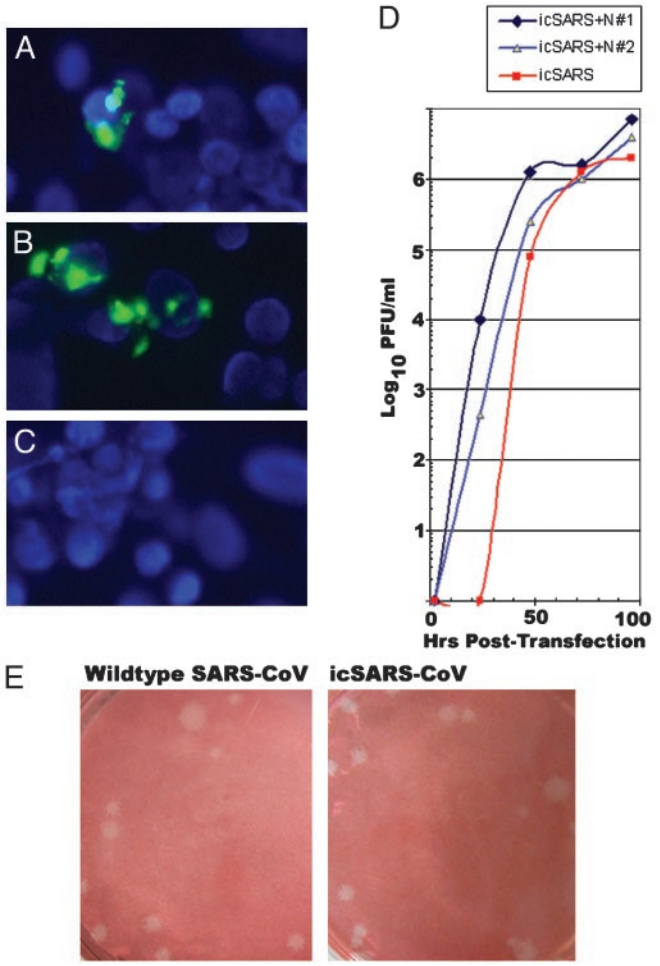

Fig. 2. SARS-CoV full-length transcripts are infectious. Full-length transcripts, in the presence or absence of SARS N transcripts, were electroporated into BHK cells and overlaid with susceptible VeroE6 cells. A portion of the cells was examined by fluorescent Ab staining. (*A*) Cultures transfected with SARS-CoV full-length transcripts. (*B*) SARS full-length transcripts plus N transcripts. (*C*) Uninfected control. (*D*) Virus growth was determined for the first 96 h after transfection by plaque assay; icSARS transcripts alone (■) and icSARS plus N transcripts, trials 1 (◆) and 2 (△). (*E*) icSARS-CoV and WT SARS-CoV plaques in Vero E6 cells.

Rescue of Molecularly Cloned SARS-CoV. To build a full-length SARS-CoV cDNA, subclones were digested with the appropriate restriction enzymes, ligated together, and used as template for *in vitro* transcription with the T7 RNA polymerase. Because N transcripts enhance infectivity of TGEV and MHV transcripts (17, 22), and are essential for IBV transcript infectivity (20), SARS-CoV full-length transcripts were tested alone or mixed with SARS-CoV N transcripts and electroporated into cells. Within 48 h, SARS-CoV-infected cells were detected by fluorescent Ab staining (Fig. 2 *A–C*). Rescued recombinant virus (icSARS-CoV) titers approached 1.0×10^6 plaque-forming units/ml at 48 h after infection in the mixed transcript trans-

MICROBIOLOGY

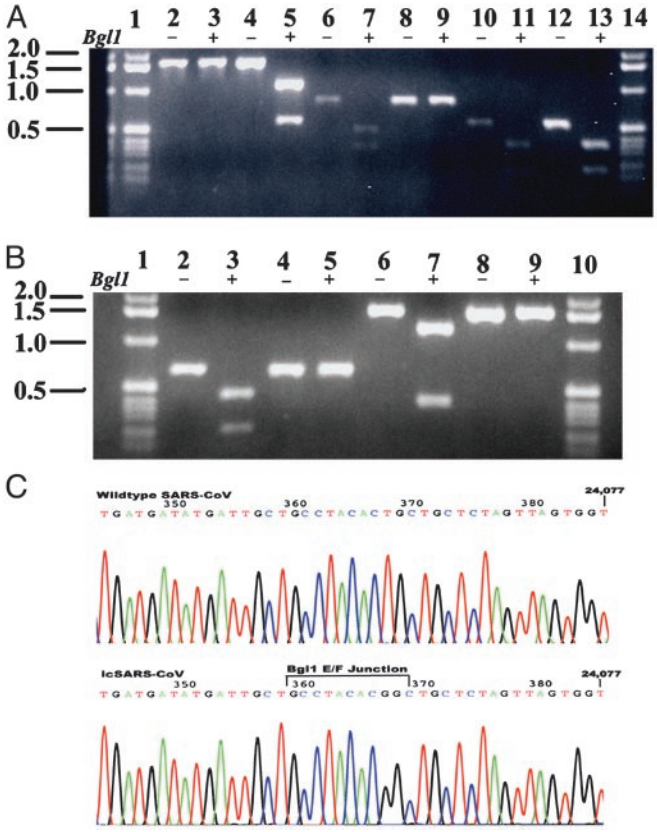

Fig. 3. icSARS-CoV marker mutations. cDNAs spanning the different *Bgl*I junctions were amplified from WT and icSARS-CoV-infected cells. The fragments were purified, and a portion was digested with *Bgl*I and separated in 1.2% agarose gels. (*A*) icSARS-CoV (lanes 2, 3, 6, 7, 10, and 11) and WT SARS-CoV (lanes 4, 5, 8, 9, 12, and 13). Lanes 2–5, a 1,668-nt amplicon (nucleotide positions 1007–2675) digested with *Bgl*I (lanes 3 and 5); lanes 6–9, a 799-nt amplicon spanning the SARS-CoV B/C junction (positions 8381–9180) digested with *Bgl*I (lanes 7 and 9); lanes 10–13, a 544-nt amplicon (positions 11,721–12,265) spanning the SARS-CoV C/D junction digested with *Bgl*I (lanes 11 and 13). Lanes 1 and 14, a 1-kb ladder. (*B*) WT SARS (lanes 4, 5, 8, and 9); icSARS-CoV (lanes 2, 3, 6, and 7). Lanes 2–5, a 652-nt amplicon spanning the SARS-CoV D/E junction digested with *Bgl*I (lanes 3 and 5); lanes 6–9, a 1,594-nt amplicon (positions 23,665–25,259) spanning the SARS-CoV E/F junction digested with *Bgl*I (lanes 7 and 9). Lanes 1 and 10, a 1-kb ladder. (*C*) The 1,594-nt SARS E/F junction-containing amplicon was subcloned and sequenced, demonstrating the mutations introduced within the icSARS-CoV.

fected cultures (Fig. 2*D*). Recombinant viruses were also detected in cultures transfected with genome-length SARS-CoV transcripts alone, but titers were reduced. SARS-CoV N transcripts may enhance but are not essential for infectivity of SARS full-length transcripts. Molecular cloned viruses produced similar sized plaques as WT SARS-CoV Urbani (Fig. 2*E*).

icSARS-CoV Marker Mutations. Rescued icSARS-CoV, but not WT SARS-CoV, should contain several *Bgl*I sites that were engineered as junctions between the SARS B/C, D/E, and E/F subclones and lack the *Bgl*I site at nucleotide position 1577. Intracellular RNA was isolated from infected cultures, RT-PCR amplified by using primer pairs flanking these various sites, and subjected to restriction-fragment-length polymorphism analysis with *Bgl*I. Clearly, icSARS-CoV contained the marker mutations inserted within and between the component clones (Fig. 3 *A* and *B*). Selected amplicons were cloned and sequenced, demonstrating that the icSARS-CoV originated from transcripts derived from the full-length cDNA construct (Fig. 3*C*).

Phenotype of Rescued icSARS-CoV. Recombinant icSARS-CoV replicated as efficiently as WT Urbani, but slightly less efficiently than the Tor-2 and Tor-7 SARS-CoV isolates (Fig. 4*A*). All viruses replicated to titers of $\approx 1–5 \times 10^7$ within ≈24–48 h after infection. icSARS-CoV subgenomic mRNAs should contain a common ≈72-nt leader RNA sequence, which is derived from the 5′ end of the genome. Intracellular RNA was isolated from Urbani WT and icSARS-CoV-infected cultures. Primer pairs were derived from the leader RNA sequence and from various locations at the 3′ end of the genome. After RT-PCR amplification of leader-containing amplicons, sequence analysis indicated that eight WT and icSARS-CoV subgenomic transcripts originated at identical CS sites, defined by the core sequence ACGAAC (Fig. 4*B*). This sequence represents a truncation of the AAACGAAC CS site that had been predicted by Rota *et al.* (8) and is different from the group I, II, and III CoV CS, CUAAAC (TGEV), UCTAAAC (MHV), and CUUAACAA (IBV), respectively. Although some previous studies suggested that the SARS E protein and ORF X3 might be expressed from multicistronic mRNA, our findings indicate that independent transcripts are initiated at the core CS ACGAAC noted at nucleotide positions 26109 for E transcripts and 26913 for ORF X3 transcripts, respectively (Fig. 4*B*). Several may encode two or more ORFs (Fig. 4*B*) (11). Using 5′ RACE, SARS N transcripts contained an identical 72-nt 5′ leader RNA sequence derived from the 5′ end of the genome (data not shown).

***In Vitro* Inhibition of SARS-CoV Replication.** During MHV and foot and mouth disease virus infection, the cysteine proteinase inhibitor E64-d blocks replicase polyprotein processing, thereby inhibiting viral RNA synthesis and growth (12). E64-d is noncytotoxic to cells and does not inhibit cellular RNA synthesis. Moreover, removal of the E64-d allows recovery of virus replication (12). To determine whether icSARS-CoV was susceptible to the inhibitory effects of E64-d, growth comparisons were performed in the presence and absence of drug. In the absence of E64-d, WT and icSARS-CoV grew to equivalent titers of $\approx 1.0 \times 10^7$ plaque-forming units/ml after 24–48 h after infection. Untreated, infected VeroE6 cells showed extensive cytopathic effect with cell rounding and loss at 72 h (Fig. 4*D*). Treatment of cells with a single dose of E64-d at 1 h after infection resulted in a significant ≈3–4 log reduction in virus yield for both WT and icSARS-CoV at 24 and 48 h after infection, respectively, with concomitant reductions in viral cytopathic effect at 72 h and healthy intact monolayers (Fig. 4 *C* and *D*). Under similar conditions, MHV replication was also reduced by ≈3.0 logs, from 3.0×10^7 to 1.5×10^4 at 10 h, but rebounded to 1.0×10^7 plaque-forming units/ml by 24 h after infection. Thus, the replication of icSARS-CoV appeared to be inhibited by a single dose of E64-d for a longer duration than MHV. Details of E64-d effects on SARS polyprotein processing will be reported in more detail elsewhere.

Discussion

It is hypothesized that the SARS-CoV emerged from exotic animals in China. Although no one can accurately predict the future impact of SARS-CoV on the global community, the past 25 years has seen the emergence and global spread of several new pathogenic CoVs in animals (23–25). Coupled with *in vitro* findings, CoVs are serious emerging pathogens capable of rapid evolution, cross species transmission, and colonization of new host species (26, 27). Given the exigency of the SARS-CoV outbreak, the availability of a full-length cDNA will provide a genetic approach to manipulate the SARS-CoV genome for vaccine development and to explore the complexity of the genome. The SARS replicase contains several predicted enzymatic activities and undefined domains whose function in rep-

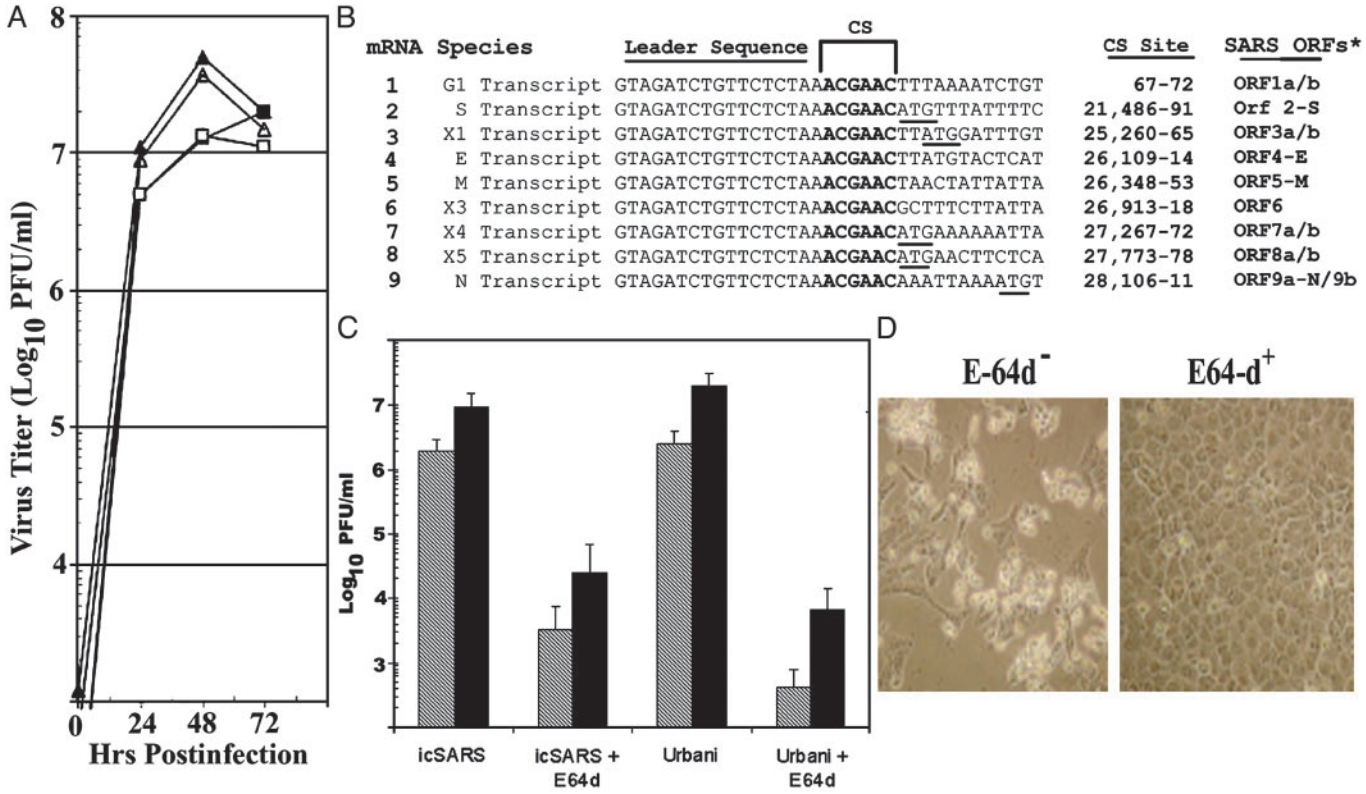

Fig. 4. Phenotype comparisons between WT and icSARS-CoV. Cultures of cells were infected with an multiplicity of infection of 0.1. At 1 h, cultures were treated with E64-d at a concentration of 500 μg/ml, and virus titers were determined by plaque assay in VeroE6 cells (*C*). (*A*) Growth of Urbani (■), icSARS (□), and the Tor-2 (▲) and Tor-7 (△) CoVs. (*B*) Leader-containing transcripts encoding various icSARS-CoV subgenomic ORFs. *, predicted ORFs classified by using standard CoV nomenclature (11). (*C*) Growth of icSARS and Urbani SARS-CoV in the presence or absence of E64-d. Hatched bars, 24-h titers; black bars, 48-h titers. (*D*) Urbani SARS-CoV-infected cells at 72 h after infection.

lication remain largely unexplored but may represent targets for antiviral intervention (11).

Effective biodefense and control of emerging infections requires rapid response methodologies for developing safe and effective vaccines and therapeutics. For SARS-CoV, the combination of high-throughput screening and class IIS restriction endonucleases streamlined the isolation and assembly of consensus cDNA fragments and resulted in recovery of recombinant SARS-CoV within 2 mo of obtaining viral RNA. We have hypothesized that these approaches could be applied to any newly emerging RNA or DNA virus pathogen and also allows the assembly of large genes and genomes by ligation of synthetic oligonucleotides *in vitro* (17, 18).

We have constructed full-length cDNAs of representative group I and group II CoVs. As with MHV and TGEV, N transcripts enhance recovery of rescued viruses (17,18). Although the exact mechanism is unknown, data from our laboratory indicate that a functional N ORF is critical. N protein may enhance the translation of viral mRNAs, protect the viral genome, or enhance subgenomic transcription (K.M.C., B.Y., A. C. Sims, and R.S.B., unpublished observation). In agreement with earlier reports (11), icSARS-CoV-infected cells contain genome length and at least eight subgenomic mRNAs encoding a common 72-nt leader RNA sequence fused at a common core CS "ACGAAC." The CS core sequence is only encoded at these critical sites for subgenomic transcription. Several of these subgenomic mRNAs (mRNA 3, 7, 8, and 9) may be functionally multicistronic, but the function of these downstream group-specific ORFs remains unknown. As high homology is necessary for leader/body CS fusion and efficient synthesis of subgenomic mRNAs, we predict that the previously undescribed SARS transcriptional regulatory sequence may provide a formidable obstacle against intergroup RNA recombination, especially at the 3′ end of the genome.

The SARS full-length cDNA may allow for the development of live candidate vaccine strains that contain defined attenuating mutations. Generating safe and effective CoV vaccines has proven challenging in both animals and humans because these viruses often replicate at mucosal surfaces and the most severe forms of disease oftentimes occur in newborn animals. Vaccines have not been developed for the human CoVs HCV-229E and HCV-OC43 because of limited disease severity and short-term protective immunity. Killed-virus vaccine candidates have not proven very successful against TGEV, feline infectious peritonitis virus, and IBV. Live attenuated and recombinant virus vaccines have proven effective against TGEV, MHV, and IBV (32–37). However, feline infectious peritonitis virus vaccination with killed, recombinant or live-attenuated virus results in the production of anti-S Abs, leading to disease enhancement and death after virus challenge (38, 39). Although long-lived mucosal immunity, immune enhancement, and recombination with existing strains are potential problems facing the development of an efficacious SARS vaccine, several animal vaccine approaches have proven successful and most SARS patients develop immune responses and recover (2, 4, 40, 41).

Although at an early stage of development, Fouchier *et al.* (42) infected four macaques simultaneously through the conjunctiva, nose, and trachea. The animals became lethargic at 3 d, and virus was detected in all four infected animals which seroconverted. The two animals infected at the higher dose were autopsied at 6 d after infection and had lesions in the lung similar to those in infected humans. The testing of molecularly cloned icSARS-

CoV as an innoculum in primates should provide further evidence for a CoV etiology of SARS. Further refinement of the nonhuman primate model, coupled with a full-length cDNA clone for the introduction of precise modifications into rescued icSARS-CoV, should allow for the development of candidate vaccines for the clinic. For example, deletion of the nonconserved, group-specific ORFs encoded within the last one-third of the genome was not detrimental CoV replication *in vitro*, but viruses were attenuated *in vivo* (22, 28, 29). These ORFs can also be replaced with foreign genes, providing for heterologous gene expression from recombinant viruses and from single-hit replicon particles (22, 30, 31). Although speculative, some of the SARS group-specific ORFs may also encode luxury functions that attenuate pathogenesis *in vivo* but may have little impact on *in vitro* replication.

The availability of a SARS-CoV infectious clone will provide a tool to study candidate antiviral agents. The current data indicate that the cysteine proteinase inhibitor E64-d may inhibit SARS virus replication at any time during infection. The demonstrated ability of E64-d in the MHV model to inhibit multiple proteinases suggests that it might be less susceptible to virus escape by mutations in individual proteinases (12). The recent description of the structure of the CoV 3C-like proteinase (44) will guide targeted genetic studies of susceptibility to candidate antivirals and the evolution of drug resistance. In addition, the replicase gene comprises two-thirds of the SARS-CoV genome and encodes many proteins of unknown function. The availability of a full-length cDNA of the SARS genome should allow for genetic manipulation of the replicase gene providing new insights into the role of specific proteolytic cleavages and replicase proteins during viral replication.

We thank Laura Livingstone (University of North Carolina Lineberger Comprehensive Cancer Center DNA sequencing facility) for providing rapid, high-throughput sequence analysis. We also thank Quing Yang (Lineberger Comprehensive Cancer Center Nucleic Acid Core Facility) for the rapid production of high-quality oligodeoxynucleotide primers and Amy Sims for critical reading of the manuscript. This work was supported by National Institutes of Health Grants AI23946, GM63228 (to R.S.B.), and AI26603 (to M.R.D.). The research was supported by the Carolina Vaccine Institute at the University of North Carolina, Chapel Hill.

1. Tsang, K. W., Ho, P. L., Ooi, G. C., Yee, W. K., Wang, T., Chan-Yeung, M., Lam, W. K., Seto, W. H., Yam, L. Y., Cheung, T. M., *et al.* (2003) *N. Engl. J. Med.* **348,** 1977–1985.
2. Lee, N., Hui, D., Wu, A., Chan, P., Cameron, P., Joynt, G. M., Ahuja, A., Yung, M. Y., Leung, C. B, To, K. F., *et al.* (2003) *N. Engl. J. Med.* **348,** 1986–1994.
3. Peiris, J. S, Chu, C. M., Cheng, V. C., Chan, K. S., Hung, I. F., Poon, L. L., Law, K. I., Tang, B. S., Hon, T. Y, Chan, C. S., *et al.* (2003) *Lancet* **361,** 1767–1772.
4. Poutanen, S. M., Low, D. E., Henry, B., Finkelstein, S., Rose, D., Green, K., Tellier, R., Draker, R., Adachi, D., Ayers, M., *et al.* (2003) *N. Engl. J. Med.* **348,** 1995–2005.
5. Peiris, J. S., Lai, S. T., Poon, L. L., Guan, Y., Yam, L. Y., Lim, W., Nicholls, J., Yee, W. K., Yan, W. W., Cheung, M. T., *et al.* (2003) *Lancet* **361,** 1319–1325.
6. Ksiazek, T. G., Erdman, D., Goldsmith, C., Zaki, S. R., Peret, T., Emery, S., Tong, S., Urgani, C., Comer, J. A., Lim, W., *et al.* (2003) *N. Engl. J. Med.* **348,** 1953–1966.
7. Drosten, C., Gunter, S., Preisner, W., van der Werf, S., Brodt, H. R., Becker, S., Rabenau, H., Panning, M., Kolesnikova, L., Fouchier, R. A., *et al.* (2003) *N. Engl. J. Med.* **348,** 1967–1976.
8. Rota, P. A., Oberste, M. S., Monroe, S. S., Nix, W. A., Campagnoli, R., Icenogle, J. P., Penaranda, S., Bankamp, B., Maher, K., Chen, M. H., *et al.* (2003) *Science* **300,** 1394–1398.
9. Marra, M. A., Jones, S. J., Astell, C. R., Holt, R. A., Brooks-Wilson, A., Butterfield, Y. S., Khattra, J., Asano, J. K., Barber, S. A., Chang, S. Y., *et al.* (2003) *Science* **300,** 1399–1404.
10. Ruan, Y. J., Wei, C. L., Ee, L. A., Vega, V. B., Thoreau, H., Yun, S. T., Chia, J. M., Ng, P., Chiu, K. P., Lim, L., *et al.* (2003) *Lancet* **361,** 1779–1785.
11. Snijder, E. J, Bredenbeek, P. J., Dobbe, J. C., Thiel, V., Ziebuhr, J., Poon, L. L. M., Guan, Y., Rozanov, M., Spaan, W. J. M. & Gorbalenya, A. E. (2003) *J. Mol. Biol.* **331,** 991–1004.
12. Kim, J. C, Spence, R. A., Currier, P. F., Lu, X. T. & Denison, M. R. (1995) *Virology* **208,** 1–8.
13. Kanjanahaluethai, A., Jukneliene, D. & Baker, S. C. (2003) *J. Virol.* **77,** 7376–7382.
14. Gorbalenya, A. E., Koonin, E. V. & Lai, M. M. C. (1991) *FEBS Lett.* **288,** 201–205.
15. Lu, X. T., Sims, A. C. & Denison, M. R. (1998) *J. Virol.* **72,** 2265–2271.
16. von Grotthuss, M., Wyrwicz, L. S. & Rychlewski, L. (2003) *Cell* **113,** 701–702.
17. Yount, B., Denison, M. R., Weiss, S. R. & Baric, R. S. (2002) *J. Virol.* **76,** 11065–11078.
18. Yount, B., Curtis, C. & Baric, R. S. (2000) *J. Virol.* **74,** 10600–10611.
19. Almazon, F., Gonzalez, J. M., Penzes, Z., Izeta, A., Calvo, E., Plana-Durin, J. & Enjuanes, L. (2000) *Proc. Natl. Acad. Sci. USA* **97,** 5516–5521.
20. Casais, R., Thiel, V., Siddell, S. G., Cavanagh, D. & Britton, P. (2001) *J. Virol.* **75,** 12359–12369.
21. Thiel, V., Herold, J., Schelle, B. & Siddell, S. G. (2001) *J. Gen. Virol.* **82,** 1273–1281.
22. Curtis, K. M., Yount, B. & Baric, R. S. (2002) *J. Virol.* **76,** 1422–1434.
23. Pensaert, M. B. & de Bouck, P. (1978) *Arch. Virol.* **58,** 243–247.
24. Pensaert, M., Callebaut, P. & Vergote, J. (1986) *Vet. Q.* **8,** 257–261.
25. Duarte, M., Tobler, K., Bridgen, A., Rasschaert, D., Ackermann, M. & Laude, H. (1994) *Virology* **198,** 466–476.
26. Baric, R. S., Yount, B., Hensley, L., Peel, S. A. & Chen, W. (1997) *J. Virol.* **71,** 1946–1955.
27. Baric, R. S., Sullivan, E., Hensley, L., Yount, B. & Chen, W. (1999) *J. Virol.* **73,** 638–649.
28. Fischer, F., Stegen, C. F., Koetzner, C. A. & Masters, P. S. (1998) *J. Virol.* **71,** 7885–7894.
29. de Haan, C. A, Masters, P. S, Shen, X., Weiss, S. & Rottier, P. J. (2002) *Virology* **296,** 177–189.
30. Sola, I., Alanso, S., Zuniga, S., Balasch, M., Plana-Duran, J. & Enjuanes, L. (2002). *J. Virol.* **77,** 4357–4369.
31. Ortega, J., Escors, D., Laude, H. & Enjuanes, L. (2002) *J. Virol.* **76,** 11518–11529.
32. Enjuanes, L. & van der Zeijst, B. A. M. (1995) in *The Coronaviridae*, ed. Siddell, S. G. (Plenum, New York), pp. 337–376.
33. Ladman, B. S., Pope, C. R., Ziegler, A. F., Swieczkowski, T., Callahan, C. J., Davison, S. & Gelb, J., Jr. (2002) *Avian Dis.* **46,** 938–944.
34. Saif, L. J. (1999) *Adv. Vet. Med.* **41,** 429–446.
35. van Nieuwstadt, A. P., Zetstra, T. & Boonstra, J. (1989) *Vet. Res.* **125,** 58–60.
36. Crouch, C. F., Oliver, S., Hearle, D. C., Buckley, A., Chapman, A. J. & Francis, M. J. (2000) *Vaccine* **19,** 189–196.
37. Park, S., Sestak, K., Hodgins, D. C., Shoup, D. I., Ward, L. A., Jackwood, D. J. & Saif, L. J. (1998) *Am. J. Vet. Res.* **59,** 1002–1008.
38. Rottier, P. J. (1999) *Vet. Microbiol.* **69,** 117–125.
39. Vennema, H., de Groot, R. J., Harbour, D. A., Dalderup, M., Gruffydd-Jones, T., Horzinek, M. C. & Spaan, W. J. (1997) *J. Virol.* **64,** 1407–1409.
40. Wang, X., Schnitzlein, W. N., Tripathy, D. N., Girshieck, T. & Khan, M. I. (2002) *Avian Dis.* **46,** 831–838.
41. Baron, M. D., Foster-Cuevas, M., Baron, J. & Barrett, T. (1997) *J. Gen. Virol.* **80,** 2031–2039.
42. Fouchier, R. A. M., Kuiken, T., Schutten, M., van Amerongen, G., van Doorman, G. J., van den Hoogen, B. G., Peris, M., Lim, W., Stohr, K. & Osterhaus, M. D. (2003) *Nature* **423,** 240.
43. Komatsu, K., Inazuki, K., Hosoya, J. & Satoh, S. (1986) *Exp. Neurol.* **91,** 23–29.
44. Anand, K., Ziebuhr, J., Wadhwani, P., Mesters, J. R. & Hilgenfeld, R. (2003) *Science* **300,** 1763–1767.